

CHAPTER 2

LITERATURE REVIEW

Ionic conduction that occurs in conducting ionic materials is due to the monovalent cation, such as Li^+ , Cu^+ , Ag^+ , Na^+ , K^+ and so on or anions such as F^- , Cl^- , Br^- and I^- . Only O^{2-} anion is a divalent conducting species. The materials could be crystalline, amorphous or composite. In this chapter, ionic materials with Ag^+ and Cu^+ as the cation and I^- as the anion will be discussed. Solids with high ionic conductivity at room temperature are termed as superionic solids or fast ion conductors (Bosko, 2003).

2.1 Silver ion conductors

Room temperature silver ion conductors are mainly limited to compounds based on AgI. From X-ray investigations, the unit cell of AgI consists of two silver ions. These are distributed over forty two available tetrahedral and octahedral sites. These sites correspond to a “quasi-molten” or “liquid-like” state of the silver ions which enable free movement. Neutron diffraction experiments on α -AgI indicate that the silver ions are found at tetrahedral sites and that there is a large anharmonic contribution to the thermal vibrations in the direction of the octahedral sites. This model suggested that silver ions are not completely liquid-like and the Ag^+ ions diffuses through some channel-like pathways of silver ions (Takahashi, 1978).

Silver iodide is a yellow, crystalline solid with a melting point at 552°C and boiling point at 1506°C. AgI is a chemical compound, normally used in photography, antiseptic in medicine, rainmaking as well as cloud seeding. AgI is highly insoluble in water. The crystalline structures adopted by AgI changes with temperature. At room temperature, AgI exists in the metastable γ -phase, with a zincblende structure. From room temperature to 420 K (147°C), AgI exists in the β -phase, with a wurtzite structure. Above 420 K (147°C) β -AgI undergoes transition to α -phase, with a body centered cubic structure. The transition between β and α phases represent the melting of the silver ions sublattice. Due to the high conductivity at 420 K and the possibility to 'lock' this high conducting phase at room temperature by combining AgI with other silver compounds has made AgI based superionic conductors important material for technology development.

There have been many theoretical and computer simulation studies conducted to understand the fast movement of Ag^+ ion in AgI and AgI based compounds. These include molecular dynamics and Monte Carlo simulations (Hiwatari, 1981). The results suggested that the potential functions of Ag^+ and I^- ions are very important to fit the theoretical and experimental results. According to Boyce et. al. (1977), based on extended X-ray absorption of fine structures atoms are slightly displaced from the center of the tetrahedral sites. From neutron powder diffraction analysis, McGreevy and co-workers (1992) have shown the local density and pathway for the diffusion of the Ag^+ ions. The Ag^+ ion diffusion path is in the $\langle 110 \rangle$ direction between tetrahedral sites.

Figure 2.1 shows the schematic view of ion diffusion paths in AgI. The two arrows showed the ion diffusion paths from the octahedral site to the cation vacancy. The bold arrow showed the Ag^+ ion starts to migrate along the $\langle 111 \rangle$ direction toward the cation vacancy via the centre of the tetrahedron, while the thin arrow showed an Ag^+ ion started to migrate directly toward the cation vacancy.

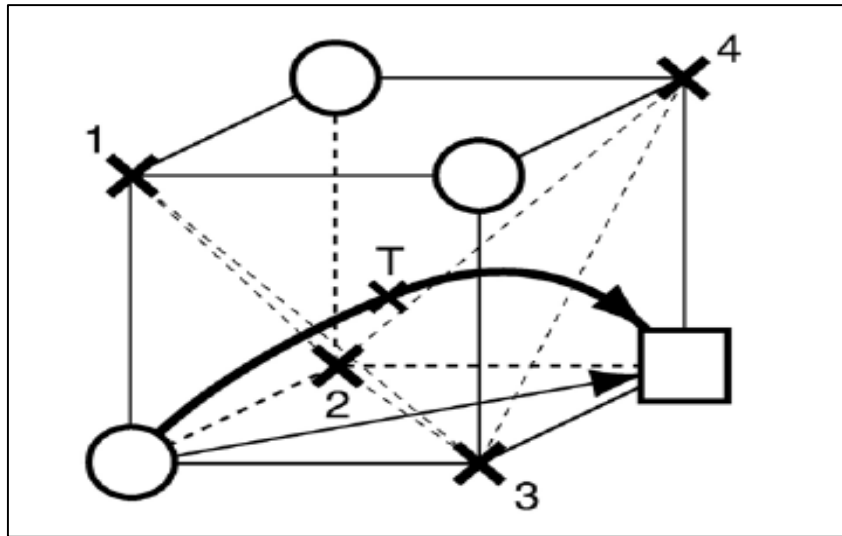


Figure 2.1: Schematic view of ion diffusion paths (Ono et.al., 2007)

As an alternative means to understand the transport of silver ions, consider Figure 2.2 that shows the cluster of Ag_6I_{10} as reported by Kowada, (2000). The structure was adopted from α -AgI crystal, since the short range structure around mobile Ag^+ ions in the AgI-based superionic conductors is similar to that in the α -AgI crystal. It can be observed from the figure that one Ag^+ ion in this cluster (see arrow) is moved from a tetrahedral site to a neighboring octahedral site through the center of a triangular plane and then is continuously moved to another tetrahedral site.

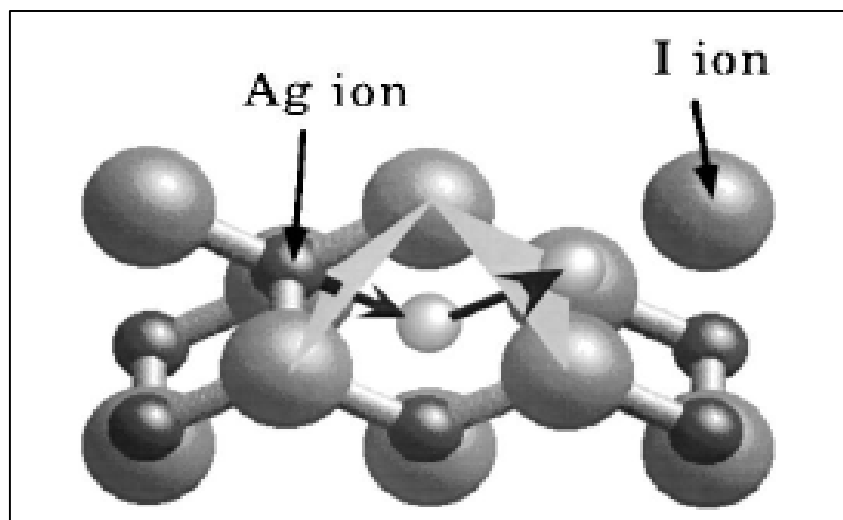


Figure 2.2: Ag_6I_{10} model cluster (Kowada et al., 2000).

2.2 Copper ion conductors

$\text{Rb}_3\text{Cu}_7\text{Cl}_{10}$ is a compound that exhibits high ion conductivity at room temperature (Takahashi, 1978). The charge carriers in these conductors have been shown to be copper (I) ions. Copper (I) ion conductors can also be synthesized by introducing organic substituted ammonium halides into the lattice of copper (I) halides (Takahashi, 1978). The high copper (I) ion conductivity can also be observed in the tricyclic ammonium halide and copper (I) halide system (Takahashi, 1978).

Copper (I) iodide or cuprous iodide has a melting point at 605°C and boiling point at 1290°C . It is very useful in a variety of applications ranging from organic synthesis to cloud seeding. CuI is white in colour. Like most two element metal halides, CuI is an inorganic polymer. CuI adopts a zincblende structure or γ -phase below 390°C (663 K). Between 390°C (663 K) and 440°C (713 K), CuI exists with the wurtzite structure (β -

phase). Above 440°C (713 K), CuI exists in the cubic structure (α -phase). The ions are tetrahedrally coordinated in the zincblende or wurtzite structure, with a Cu-I distance of 2.338 Å. CuI is a mixed ionic-electronic conductor at room temperature with predominant electron-hole conduction up to 200°C (Kumar, 2002).

In the superionic phase of CuI, the mobile ions occupy two possible sites, the tetrahedral and octahedral sites in the fcc sublattice formed by the immobile ions, as shown in Figure 2.3 (a) and (b).

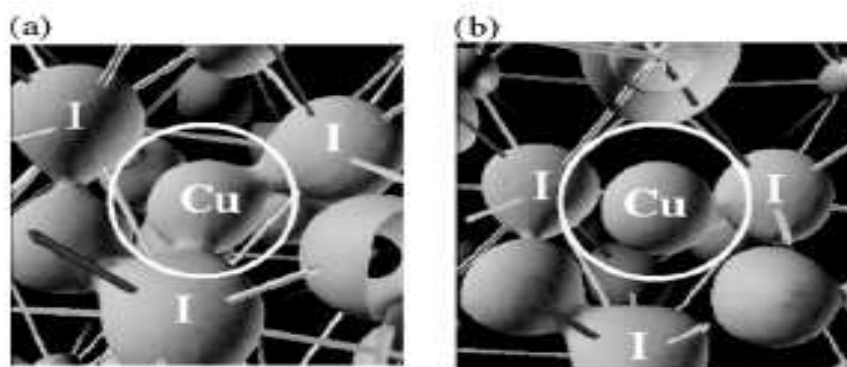


Figure 2.3: Isosurface of Cu ion at (a) tetrahedral site and (b) octahedral site (Aniya, 2005).

When the Cu ion is in the tetrahedral site, the electron density distributes between the Cu^+ ion and its neighboring I^- ions, to form covalent bonds. On the other hand, when the Cu^+ ion is at the tetrahedral site, the electron density distributes spherically around Cu^+ ions, suggesting an ionic bond (Aniya, 2005).

Figure 2.4 shows the schematic complex ion model $[\text{CuI}_8]^{7-}$ reported by (Ida, 2002). Solid dark circles denote the positions of the iodine ions and the shaded area indicates the space in which Cu^+ ions are located. It is considered the jumping models in the following two cases (Ida, 2002):

- The mobile ions jumped from tetrahedral 12(d) intra sublattice to the nearest neighbour 12(d) sublattices, where the tetrahedral 12(d) sublattice is formed by four anions and a centre of this sublattice is 12(d) site.
- The mobile ions jump from octahedral 6(b) intra sublattice to the nearest neighbour 6(b) sublattices.

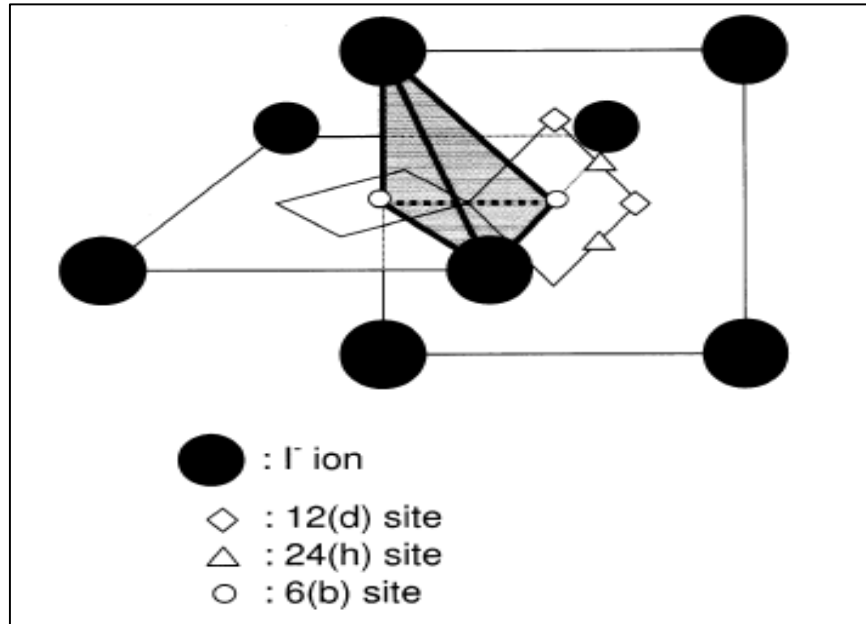


Figure 2.4: The schematic complex ion model $[\text{CuI}_8]^{7-}$ (Ida, 2002)

CuI able to form a complete set of solid solutions or mixed crystals with AgI, enabling the material property to be changed as a single component system (Senthil et. al, 2006). Introducing CuI into AgI lattice is expected to initiate and stabilize structural changes in the cation sublattice which controls the phase stability and phase transition behaviour (Kumar, 2002). This aspect has been convincingly demonstrated by Mohan and Sunandana (2004) in a systematic study of AgI-CuI solid solutions.

2.3 Silver Iodide and Copper (I) Iodide based conductors

AgI-CuI based conductors are very well-known in the past decades. Table 2.1 lists some of the AgI-CuI based conductors.

Table 2.1 AgI-CuI based conductors

AgI-CuI based conductors	σ (S cm ⁻¹)	T (K)	Reference
$x\text{CuI}\cdot(50-x)\text{AgI}-y\text{Cu}_2\text{MoO}_4\cdot(50-y)\text{CuPO}_3$	9.84×10^{-3}	298	Chowdari et.al. (1998)
$\text{Ag}_{0.3}\text{Cu}_{0.7}\text{I}$	6×10^{-6}	298	Kusakabe et. al. (1996)
80%(Ag _{0.9} Cu _{0.1} I)-20%(2Ag ₂ O•P ₂ O ₅)	8.64×10^{-3}	298	Seydei and Suthanthiraraj (1996)
40(Cu _{0.95} Ag _{0.05} I)-45(Ag ₂ O)-15(B ₂ O ₃)	2.12×10^{-3}	298	Suthanthiraraj et.al. (2001)
40(Cu _{0.75} Ag _{0.25} I)-45(Ag ₂ O)-15(V ₂ O ₅)	8.4	295	Suthanthiraraj et. al., (2001)
40(Cu _{0.75} Ag _{0.25} I)-40(Ag ₂ O)-20(V ₂ O ₅)	1.28×10^{-2}	295	Suthanthiraraj et. al.(2002)
35(Cu _{0.95} Ag _{0.05} I)-32.5(Ag ₂ O)-32.5(CrO ₃)	1.1×10^{-3}	295	Murugesan et. al.(2002)
40(Cu _{0.75} Ag _{0.25} I)-30(Ag ₂ O)-30(SeO ₂)	1.4×10^{-3}	295	Murugesan et. al. (2002)

2.4 Conductivity studies

2.4.1 D.C conductivity

It is well understood that d.c measurements provide information concerning conduction process in metal-iodide-metal and metal-semiconductor-metal structures, and identification of electrode limited and/or bulk limited processes may be made (Ondo-Ndong, 2003). Such identification is made by varying several parameters including the type of metal electrodes, strength of the applied electric field, and sample temperatures.

It is reported by Murugesan et. al. 2002 that the electrical conductivity measurements were carried out in the temperature range 295 K to 445 K by complex impedance analysis over the frequency range 20 Hz to 1 MHz. The room temperature electrical conductivity (σ_{RT}) values for the samples of different compositions in the system are found to be of the order of 10^{-4} to 10^{-3} Scm⁻¹. Figure 2.5 depicted the variation of $\log(\sigma T)$ with inverse of temperature ($1/T$) obtained for five different samples, namely $x = 0.05, 0.10, 0.15, 0.20$ and 0.25 respectively. The sudden increase in conductivity observed around 420 K for all samples indicates the presence of AgI which undergoes β to α phase transition at this temperature (Chandra, 1981).

In the light of the facts, it is reasonable to assume that crystalline AgI is the predominant cause of the abrupt change observed in conductivity around 420 K, although the magnitude of the discontinuity does not appear to change much with the varied composition. This trend may be attributed to the fact that crystalline AgI is present in all three compositions.

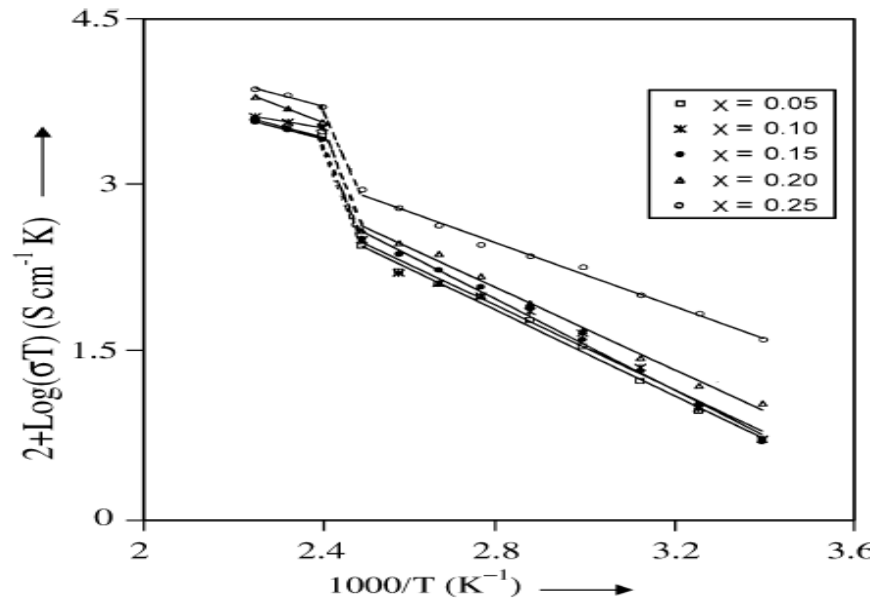


Figure 2.5: Variation of $\log(\sigma T)$ with inverse of temperature ($1/T$) for the different samples of the system $35(\text{Cu}_{1-x}\text{Ag}_x\text{I})-32.5(\text{Ag}_2\text{O})-32.5(\text{CrO}_3)$, where $0.05 \leq x \leq 0.25$ (Murugesan, 2002).

Figure 2.6 depicts plots of d.c conductivity (σ_{dc}) reported by Kumar et. al. (2003).

The conductivity values were extracted from the analysis of impedance spectra. An abrupt increase in the conductivity indicates the γ to α phase transition. The small but clear hump around 100°C (2.75 K^{-1}) is reasonably attributed to the interfacial phase transition aided by the small free energy difference between the competing β - and γ -phases of AgI , randomly distributed in the samples.

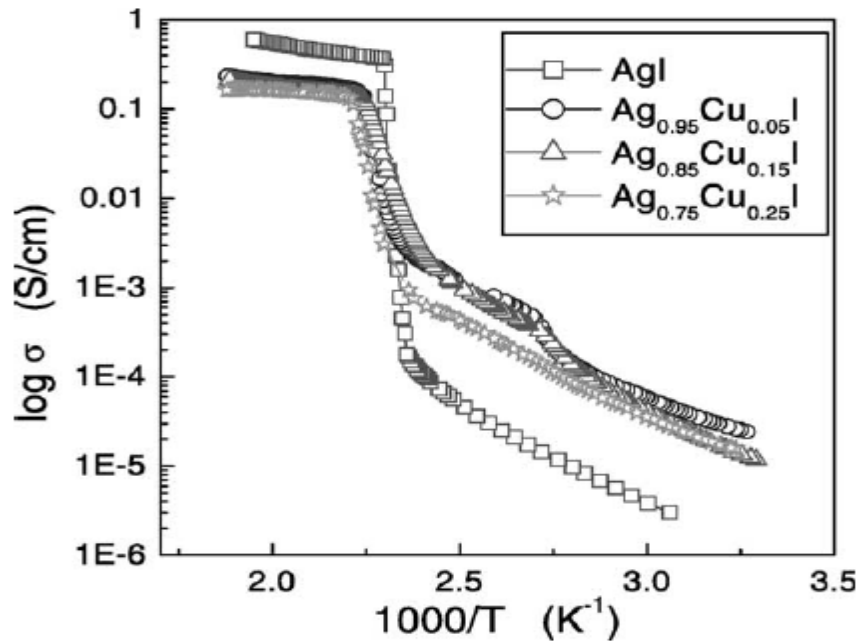


Figure 2.6: Plot of temperature dependence of the d.c. conductivity for the $\text{Ag}_{1-x}\text{Cu}_x\text{I}$ solid solutions along with pure AgI. (Kumar et. al., 2003)

Figure 2.7 shows ionic conductivity of Ag-rich of the AgI-CuI system reported by Kumar et. al.(2006). Here, the undoped AgI shows a sharp conductivity jump with the minimum temperature width. Upon progressive doping with Cu, the jump becomes less sharp with the transition occurring over a range of temperatures. Thus, the phase diagram clearly shows the low temperature single phase (γ), the intermediate temperature mixed phase ($\gamma+\alpha$) and the high temperature phase (α). This observation of mixed phase is interesting because from the AgI phase diagram, the γ -phase is apparently not stable beyond 403 K (Mellander, 1982). Thus, the mixed phase contributes through the entropy of mixing to the stability of the γ -phase in undoped AgI. These mixed phases are possibly quasi-homogeneous composites (Kumar, 2006).

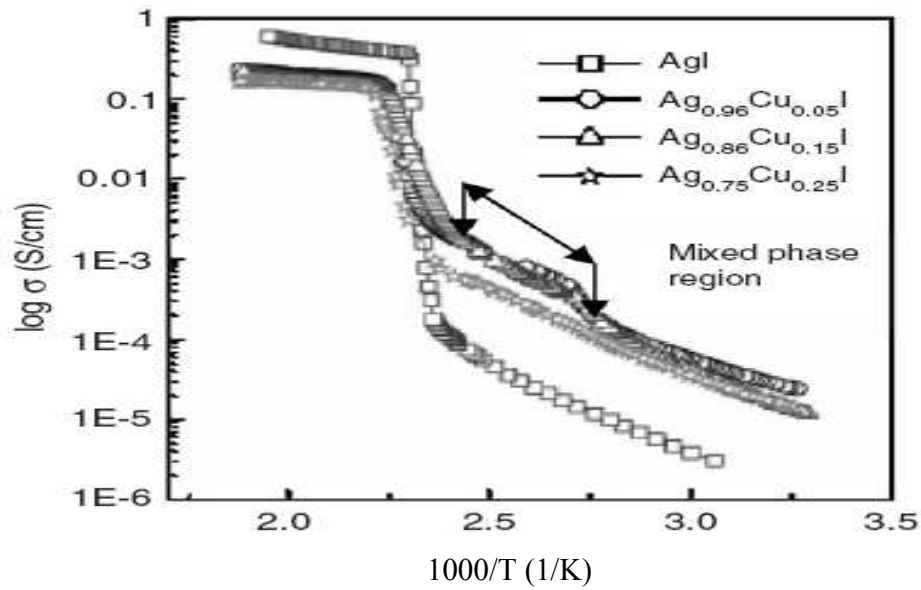


Figure 2.7: Plots of conductivity of Ag-rich solid solution (Kumar, 2006).

2.4.2 A.C conductivity

A.C conductivity measurements provide information about the interior of insulator or semiconductor which is a region of relatively low conductivity even when the conduction process is electrode limited (Ondo-Ndong, 2003).

For most transition metal, the dispersion of a.c conductivity follows the equation $\sigma_{ac}(\omega) = A\omega^s$, where the frequency exponent s is less than unity. The identification of the conduction mechanism is based on both the frequency and temperature dependence of $\sigma_{ac}(\omega)$.

Different theoretical explanations for the a.c conduction in dielectric materials which contain both amorphous as well as crystalline phases have been developed to explain

the frequency and temperature dependence on σ_{ac} and s . It is necessary to specify in an iodide that the whole of an electron and its stress field is called polaron and that is the current speaking of large and small polarons. The electron associated with a large polaron moves in a band, but its mass is slightly increased. The electron associated with a small polaron is trapped by an ion (Ondo-Ndong, 2003).

Two fundamental mechanisms which have been developed are:

- The quantum mechanical tunneling (QMT) through the barrier separating two equilibrium positions (Pollack, 1961).
- The hopping of a carrier over the barrier (Elliot, 1987).

2.5 X-ray diffraction (XRD)

XRD has been traditionally used as a fingerprint method to distinguish crystalline materials. It is extensively used for structure determination in solid state physics and it is one of the most important techniques in crystallography. The wavelengths of X-rays are the same of the same order of magnitude as the distances between atoms or ions in a molecule or crystals. To effectively prevent oxidation, all measurements must be carried out under the flowing of helium atmosphere (Tyagi, 2002). The nature of AgI-CuI mixture can be investigated by using X-ray diffraction to determine whether it is amorphous or crystalline.

According to Kumar (2002), the substitution of Cu^+ with a higher polarizability and smaller ionic size than Ag^+ is to impede the crystal growth to a significant extent, thereby lowering the average crystallite size and thus reinforcing the motion sublattice to stabilize the

zincblende phase γ -AgI, the unit cell of which is smaller than that of wurtzite or β -AgI. This is the evidence from the estimates of the particle size (~ 40 - 60 nm) from the broadened (111), (220) and (311) XRD lines using the Debye-Scherrer formula.

Figure 2.8 shows the X-ray diffraction patterns for the $\text{Ag}_{1-x}\text{Cu}_x\text{I}$ ($0.05 \leq x \leq 0.25$) compounds. From the figure, the presence of sphalerite γ -AgI structure is evidenced by the dominant (111), (220) and (330) Bragg peaks. The black circles marked weak intensity peaks corresponding to the random distribution of β -AgI arising from the stacking disorder of the sample (Kumar, 2003). The presence of additional weak reflections are attributed to the co-existence of other AgI polymorphs.

According to Yoshiasa (1995), γ -AgI cannot be easily stabilized at ambient temperature. Since the γ -AgI peaks are dominant, the role of Cu^+ ions that has a higher polarizability and smaller ionic size than the Ag^+ ion is probably to reinforce the Ag^+ ion sublattice and stabilize the zincblende γ -AgI phase (Kumar, 2003). According to Rogez (2000), the smaller Cu^+ ions are not expected to be present in the crystal bulk. Thus being in the subsurface region the Cu^+ ions can further facilitate in the reduction of interfacial energies between the randomly distributed polytypes of AgI, leading to the stabilization of the smaller metastable cubic zincblende γ -AgI. The easy nanocrystalization of silver halides with Cu addition effectively reduces the effect of strained nanoparticle formation. As can be seen from Figure 2.8, Cu assists nanoparticle formation without introducing any CuI or related phases (Kumar, 2003).

Mohan et. al (2006) reported that the undoped AgI sample contains two phases: the major γ -AgI (sphalerite or zincblende structure approximately 85.55 %) phase, characterized by the XRD peaks (111), (220), (311), (400), (331), (442), and (511) [$a = 649$ pm], and the minor β -AgI (wurtzite structure, approximately 14.45 %) identified by (100), (101), (102), and (103) reflections [$a = 412$ pm, $c = 730$ pm]. The main purpose of the Cu doping is to stabilize the metastable zincblende structure of γ -AgI as well as in assisting in particle size reduction and their results are in agreement with Kumar et. al (2002).

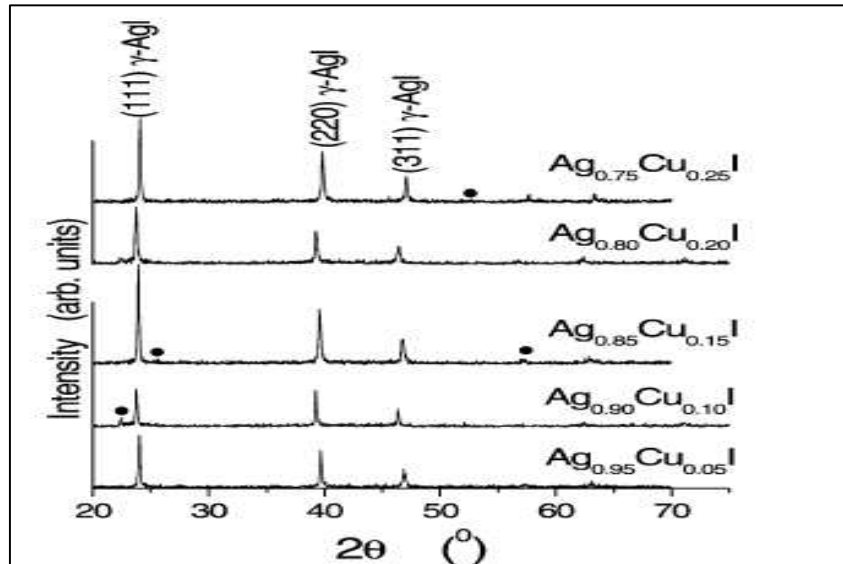


Figure 2.8: X-ray powder diffraction pattern for the $\text{Ag}_{1-x}\text{Cu}_x\text{I}$ solid for various compositions (Kumar, 2003).

Figure 2.9 depicts the representative XRD patterns of Ag-rich solid solution $\text{Ag}_{0.95}\text{Cu}_{0.05}\text{I}$ at temperature from 300 K to 723 K that was reported by Kumar et.al (2006). The transformation from the ambient γ -AgI phase to the high temperature α -AgI phase can be readily observed at temperatures above 150°C. The coexistence of the γ and α phases is clearly observed. From Figure 2.9, AgI-CuI solid solutions reveals:

- Zincblende phase of AgI is observed with the cubic lattice parameter registering a decrease with increasing of Cu content and the unit cell volume showing a corresponding change for $T < 433$ K.
- A minor wurtzite phase is also seen in the form of weak (110) reflection.

Partial substitution of Cu for Ag in AgI apparently makes the phase transition from γ -phase to α -phase occurs over a range of temperatures even in an undoped AgI. Cu substitution at 5% reinforces the cation sublattice of AgI and extends the thermal stability of the γ -AgI phase in such way that a two-phase region is created in AgI-CuI system.

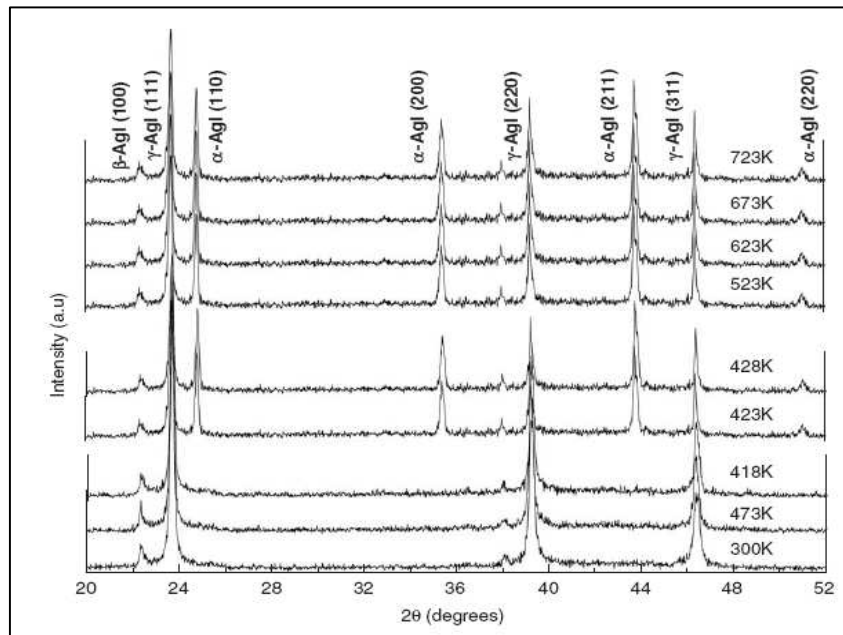


Figure 2.9: Powder XRD patterns a various temperatures for the Ag-rich $\text{Ag}_{0.95}\text{Cu}_{0.05}\text{I}$ solid solution. (Kumar, 2006).

Figure 2.10 shows the X-ray patterns for AgI-CuI solid solutions (Mohan, 2004) mechanically ground for 300 minutes. The diffractograms represent (a) pure AgI, (b) $\text{Ag}_{0.95}\text{Cu}_{0.15}\text{I}$; (c) $\text{Ag}_{0.90}\text{Cu}_{0.10}\text{I}$; (d) $\text{Ag}_{0.85}\text{Cu}_{0.15}\text{I}$; (e) $\text{Ag}_{0.75}\text{Cu}_{0.25}\text{I}$; (f) $\text{Ag}_{0.50}\text{Cu}_{0.50}\text{I}$; (g)

$\text{Cu}_{0.75}\text{Ag}_{0.25}\text{I}$; (h) $\text{Cu}_{0.85}\text{Ag}_{0.15}\text{I}$; (i) $\text{Cu}_{0.90}\text{Ag}_{0.10}\text{I}$; (j) $\text{Cu}_{0.95}\text{Ag}_{0.05}\text{I}$; and (k) pure CuI . γ - AgI nanoparticles were clearly seen upon progressively iodized Ag-Cu metastable alloy films under ambient conditions. The Bragg reflections of $\text{Ag}_{0.85}\text{Cu}_{0.15}\text{I}$ sample shows predominant peaks corresponding to the zincblende structure of γ - AgI alone. The growth of wurtzite β - AgI phase has been completely suppressed, suggesting a rapid nucleation of Cu aided γ - AgI crystallites. The sample contains unreacted Ag (111). As more Cu atoms substitute Ag in AgI , the Ag-I bond progressively shortens, thereby stabilizing the γ - AgI structure (Mohan and Sunandana, 2004).

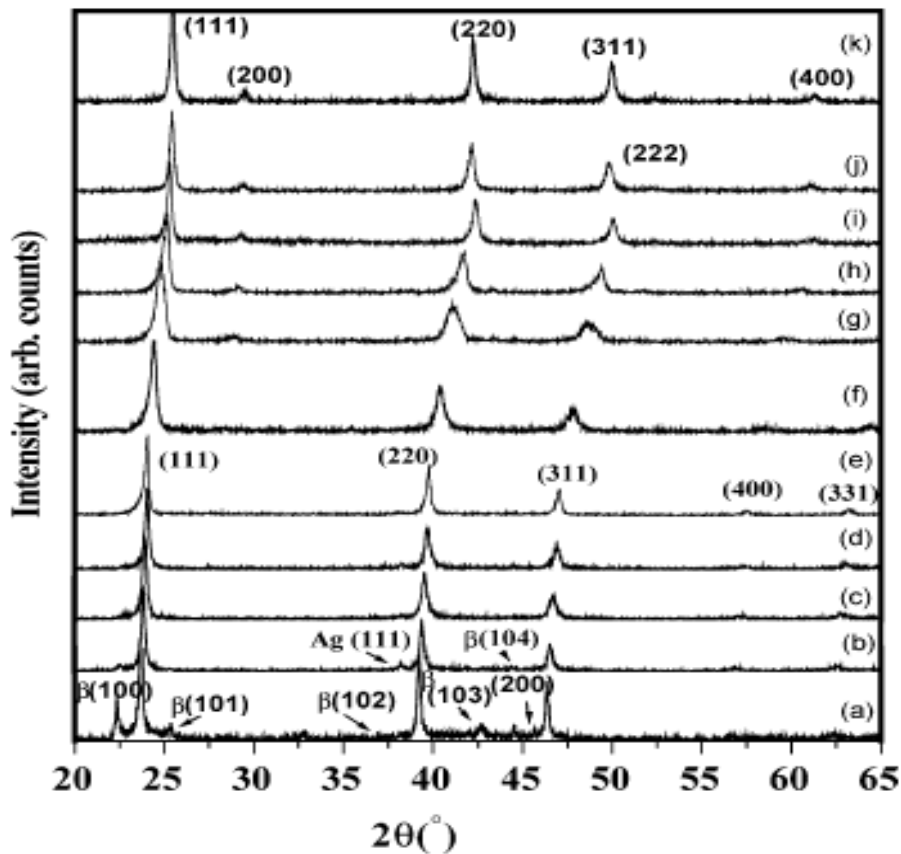


Figure 2.10: X-ray diffractograms of AgI-CuI solid solutions (Mohan, 2004).

Mohan (2002) reported the X-ray diffraction pattern of $\text{Ag}_{1-x}\text{Cu}_x\text{I}$ where $x=0.05, 0.15, 0.25$ and 0.50 . It can be observed that the undoped AgI reveals the presence of a mixture of two phases:

- The major γ -AgI (Sphalerite or Zincblende structure, approximately 95 %) phase, characterized by the XRD peaks (111), (220), (311), (400), and (331) [$a=649\text{nm}$].
- The minor β -AgI (Wurtzite structure, approximately 5 %) phase identified by (100) reflections [$a=412\text{nm}, c=130\text{nm}$].

The main purpose of Cu doping is to stabilize the metastable-zincblende structure of γ -AgI besides assisting in particle size reduction. γ -AgI nanoparticles were clearly seen upon progressively iodized Ag-Cu metastable alloy thin films under ambient conditions, which have been studied by optical absorption and photoluminescence by Kumar (2003).

$\text{Ag}_{0.95}\text{Cu}_{0.05}\text{I}$ ($x=0.05$) and one silver has β -AgI (100) with very less intensity, approximately 0.6 % and one silver line (111) with three γ -AgI lines, approximately 96.4 %. It can be observed the $\text{Ag}_{0.85}\text{Cu}_{0.15}\text{I}$ sample from the Bragg reflection that the predominant peaks corresponding to only zincblende structure of γ -AgI. The growth of wurtzite phase of β -AgI is now completely suppressed, which suggest that a rapid nucleation of γ -AgI crystallites aided by Cu. In the case of $\text{Ag}_{0.75}\text{Cu}_{0.25}\text{I}$, there is no Ag line implying complete consumption of Ag, so that the pattern corresponds to monophasic γ -AgI with sharper peaks. Furthermore, a gradually increasing of all the Bragg angles accompanied by a broadening of the (111) plane is observed upon progressive Cu addition. The lattice parameter, a (in pm) decreases linearly with Cu (wt %) in continuous manner of

0.649 to 0.626 nm. As more Cu atoms substitute Ag in AgI, the Ag-I bond progressively shortens and thereby stabilizing the γ -AgI structure.

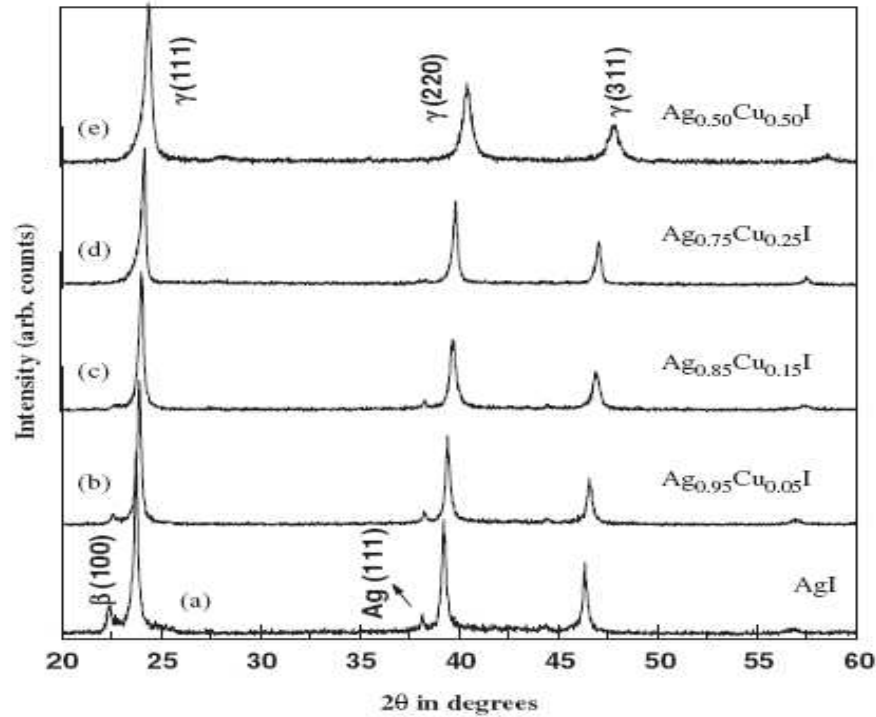


Figure 2.11: X-ray diffraction pattern of AgI-CuI based solid solutions recorded at room temperature (Mohan 2006).

2.6 Summary

The review on the results in this chapter summarized the transition phase of AgI happened at temperature about 420 K while CuI having ionic-electronic conduction up to 473 K. The graphs of $\log \sigma$ versus $1000/T$ explained the transition phase of AgI. With the sharp increases in conductivity, the transition phase of AgI is believed to be happened. The structures of AgI-CuI binary system are reviewed from the X-ray diffraction patterns and the presence of γ -AgI is evidenced by the Bragg peaks.